Mechanism of Deposition of Vanadium−Oxo Species on the "Anatase/Electrolytic Solution" Interface

K. Bourikas, I. Georgiadou, Ch. Kordulis, and A. Lycourghiotis*

Department of Chemistry, University of Patras and the Institute of Chemical Engineering and High Temperature Chemical Processes, ICE/HT-FORTH, P.O. Box 1414, GR-26500 Patras, Greece

Received: March 27, 1997; In Final Form: July 7, 1997[⊗]

The deposition of the $V^{(v)}$−oxo species on the anatase/electrolyte solution interface was studied over a wide pH and bulk concentration $V^{(v)}$ range using deposition experiments, microelectrophoresis, potentiometric titrations, and an advanced calculation procedure, further developed in the present work. It was found that the mechanism of deposition is quite complicated due to the fact that a change in pH or $V^{(v)}$ bulk concentration causes dramatic changes in the relative concentrations of the $V^{(v)}$−oxo species in the bulk solution and thus of the corresponding concentrations in the "TiO_2/electrolyte solution interface". In fact, 12 equilibria are needed in order to describe the title deposition over the pH range studied. However, a preference was found for the deposition of the monomeric $V^{(v)}$ species ($H_2VO_4^-$ and HVO_4^{2-}) with respect to the deposition of the polymeric $V^{(v)}$ species ($V_3O_9^{3-}$, $V_4O_{12}^{4-}$, $V_{10}O_{27}^{4-}$, $HV_{10}O_{28}^{5-}$). Moreover, a preference was found for deposition through adsorption (reaction) at relatively low (high) pH values on sites created by single $TiOH_2^+$ (TiOH) groups. Significant deposition has not been observed on two adjacent $TiOH_2^+$ groups or $TiOH_2^+$−O−TiOH groups. The above were quantitatively explained on the basis of an equation derived to describe the deposition. The present work was based on the two-p*K*/one-site and triple-layer models.

Introduction

It is well established that the V_2O_5/TiO_2 catalysts are very important for the selective catalytic reduction of NO by NH_3 (e.g., refs 1, 2). These catalysts are prepared using various methodologies. Among them the classical impregnation of anatase in electrolytic solutions containing $V^{(v)}$ species followed by drying and calcination is the most important (e.g., ref 3), although equilibrium deposition filtration (EDF), otherwise called "equilibrium adsorption" results of supported catalysts with relatively small size supported crystallites, studies on V_2O_5/TiO_2 catalysts prepared by EDF are not abundant in the literature.[4−9] On the other hand the preparation of the V_2O_5/TiO_2 catalysts by EDF could allow the application of a methodology for investigating the $V^{(v)}$ species formed on the anatase surface and thus the tailoring of the preparation of these catalysts. This methodology has been developed by us in the last years, in some catalytically important systems (e.g., refs 10−16).

In the present work we try by performing deposition experiments, potentiometric titrations, and microelectrophoresis and applying an advanced calculating procedure to investigate the nature and determine the concentration of the $V^{(v)}$ species formed on the anatase surface during impregnation for various values of pH and $V^{(v)}$ concentration in the bulk solution.

A second purpose of this work is to develop further the calculation procedure, recently presented,[17] in order to overcome the difficulties raised for the system under study, mainly by the dramatic change in the composition of the vanadate solution with its concentration in $V^{(v)}$.

In spite of the development of the heterogeneous models for studying the oxides/aqueous solutions interfaces (e.g., refs 18−21), our work is based on the two-p*K*/one-site model which has been recently demonstrated to describe quite well the protonation of the anatase surface[22] as well as its deposition capacity for $Cr^{(vi)}$- and $Mo^{(vi)}$−oxo species.[14,16] As to the anatase/$V^{(v)}$ species electrolyte solution interface, we adopt in the present work the well-established triple-layer model.

Experimental Section

Materials. The support used in the present study was anatase, prepared by the hydrolysis of titanium isopropoxide (Alfa, $S_{BET} = 64\ m^2\ g^{-1}$).[23]

Ammonium vanadate (NH_4VO_3) was used for the preparation of the solutions necessary for deposition as well as for the potentiometric titrations and microelectrophoresis experiments. Ammonium nitrate (Riedel de Haen, 99%) was used for the preparation of the aqueous solutions of the background electrolyte employed in the present work as well as for regulating the ionic strength of the vanadate solutions used in the deposition experiments.

Deposition Experiments. Equilibrium deposition experiments were performed at 25.0 ± 0.1 °C, ionic strength 0.1 M, adjusted by ammonium nitrate, over a pH range between 4.5 and 8.0. In each experiment 0.03 g of the support was suspended in 0.014 dm^3 of vanadate solution of various concentrations, ranging between 6×10^{-4} and 8×10^{-3} mol $V^{(v)}\ dm^{-3}$. Details on the experimental procedure have been reported elsewhere.[24−31]

The equilibrium concentration of $V^{(v)}$, C_{eq} (mol dm^{-3}), was determined spectrophotometrically (Varian Cary 219 UV/VIS) at 392 nm,[32] and the respective surface concentration, Γ (mol m^{-2}), was determined using a well-known equation.[24,25]

Potentiometric Titrations. The experimental procedure concerning the potentiometric titrations of electrolyte solutions or suspensions has been reported elsewhere.[25−29] This procedure allows the determination of the amount of the hydrogen ions consumed (H_c^+) for the protonation of the surface TiO^- and TiOH groups as well as in the equilibria taking place in the solution. Details concerning this determination have been reported elsewhere.[30,31]

* To whom correspondence should be addressed.

[⊗] Abstract published in *Advance ACS Abstracts,* August 15, 1997.

S1089-5647(97)01078-X CCC: $14.00

TABLE 1: Values of Concentration of the $V^{(v)}$ Species$_j$ in the Bulk Solution[a]

	pH					
species	4.5	5.0	6.0	6.5	7.0	8.0
$[H_2VO_4^-]_b$	5.34×10^{-5}	1.04×10^{-4}	3.97×10^{-4}	4.14×10^{-4}	4.19×10^{-4}	4.12×10^{-4}
$[HVO_4^{2-}]_b$	1.67×10^{-8}	1.03×10^{-7}	3.92×10^{-6}	1.29×10^{-5}	4.13×10^{-5}	4.07×10^{-4}
$[VO_4^{3-}]_b$	1.48×10^{-16}	2.88×10^{-15}	1.10×10^{-12}	1.15×10^{-11}	1.16×10^{-10}	1.14×10^{-8}
$[V_2O_7^{4-}]_b$	5.11×10^{-16}	1.93×10^{-14}	2.82×10^{-11}	3.07×10^{-10}	3.14×10^{-9}	3.04×10^{-7}
$[V_3O_9^{3-}]_b$	2.11×10^{-6}	1.55×10^{-5}	8.62×10^{-4}	9.80×10^{-4}	1.01×10^{-3}	9.66×10^{-4}
$[V_4O_{12}^{4-}]_b$	1.03×10^{-7}	1.47×10^{-6}	3.12×10^{-4}	3.70×10^{-4}	3.87×10^{-4}	3.63×10^{-4}
$[V_{10}O_{27}^{4-}]_b$	2.77×10^{-5}	2.15×10^{-5}	1.41×10^{-5}	2.16×10^{-8}	2.42×10^{-11}	2.06×10^{-17}
$[HV_{10}O_{28}^{5-}]_b$	3.03×10^{-6}	7.44×10^{-6}	4.88×10^{-5}	2.36×10^{-7}	8.36×10^{-10}	7.12×10^{-15}
$[V_{10}O_{28}^{6-}]_b$	1.39×10^{-9}	1.08×10^{-8}	7.10×10^{-7}	1.09×10^{-8}	1.22×10^{-10}	1.04×10^{-14}

[a] The concentrations are expressed in mol dm^{-3} and correspond to the plateau of the respective isotherms of deposition.

By determining the value of H_c^+ in selected solutions and suspensions, the hydrogen ions consumed exclusively for the protonation of the surface TiO^- and TiOH groups in the presence and absence of vanadate ions may be determined.

Microelectrophoresis. Microelectrophoretic mobility measurements of TiO_2 suspensions at room temperature allowed the determination of the ζ-potential, namely, the potential at the shear plane of the double layer. Details on the experimental procedure followed have been reported elsewhere.[25]

A First Approach to the Deposition Model

Composition of the Impregnating Solution. The following equilibria occur in the impregnating solution.

$$VO_4^{3-} + H^+ \overset{K_A'}{\longleftrightarrow} HVO_4^{2-} \quad (1a)$$

$$HVO_4^{2-} + H^+ \overset{K_B'}{\longleftrightarrow} H_2VO_4^- \quad (1b)$$

$$2HVO_4^{2-} \overset{K_C'}{\longleftrightarrow} V_2O_7^{4-} + H_2O \quad (1c)$$

$$3H_2VO_4^- \overset{K_D'}{\longleftrightarrow} V_3O_9^{3-} + 3H_2O \quad (1d)$$

$$4H_2VO_4^- \overset{K_E'}{\longleftrightarrow} V_4O_{12}^{4-} + 4H_2O \quad (1e)$$

$$10H_2VO_4^- + H^+ \overset{K_F'}{\longleftrightarrow} V_{10}O_{27}^{4-} + 13H_2O \quad (1f)$$

$$V_{10}O_{27}^{4-} + H_2O \overset{K_G'}{\longleftrightarrow} HV_{10}O_{28}^{5-} + H^+ \quad (1g)$$

$$HV_{10}O_{28}^{5-} \overset{K_H'}{\longleftrightarrow} V_{10}O_{28}^{6-} + H^+ \quad (1h)$$

The concentration of each of the $V^{(v)}$−oxo species at a given pH and total $V^{(v)}$ concentration was calculated from equilibria 1a−1h. The required K_A', K_B', ... K_H' values were obtained from the literature.[33,34] A computer program called SURFEQL[35] has been used in the present work to perform this calculation. It was found that under our experimental conditions [pH range 4.5−8.0, concentration range 6×10^{-4} to 8×10^{-3} M $V^{(v)}$], the $H_2VO_4^-$, HVO_4^{2-}, $V_3O_9^{3-}$, $V_4O_{12}^{4-}$, $V_{10}O_{27}^{4-}$, and $HV_{10}O_{28}^{5-}$ species are present in the impregnating solution (see Table 1). Therefore, these species should be taken into account when we shall write down the tentative deposition model.

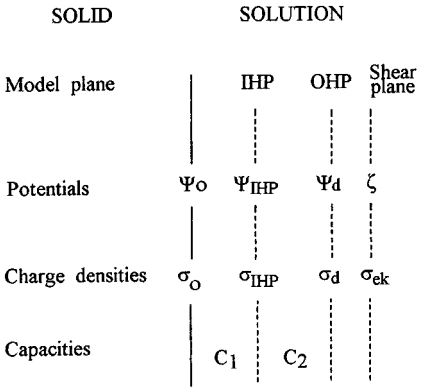

Figure 1. Structure of the electrical double layer. Triple-layer model.

Part of the Double Layer Where the Adsorbed Species Are Located. As mentioned in the Introduction, it has been shown that the "2p*K*/one-site model" [26,27,36−38] describes very well the charging of the support surface.[22] Therefore, we may write the following equilibria.

$$TiOH_2^+ \overset{K_1^{int}}{\longleftrightarrow} TiOH + H_s^+ \quad (2a)$$

$$TiOH \overset{K_2^{int}}{\longleftrightarrow} TiO^- + H_s^+ \quad (2b)$$

$$H_s^+ \leftrightarrow H_b^+ \quad (2c)$$

$$H_2O \overset{K_w}{\longleftrightarrow} H_b^+ + OH_b^- \quad (2d)$$

By $TiOH_2^+$, TiOH, and TiO^- we denote, respectively, the protonated, neutral, and deprotonated surface hydroxyls. The subscripts s and b stand for the surface and the bulk solution, respectively. The values of the surface acidity constants have been recently determined in the absence of the $V^{(v)}$−oxo species in the impregnating solution.[22] These values are not expected to be changed due to the presence of the $V^{(v)}$−oxo species. Therefore, using these values, SURFEQL may be applied for determining the concentration of the various types of surface hydroxyls in both the absence and presence of the $V^{(v)}$−oxo species in the impregnating suspension.

It is also well-known that in the presence of the ions to be deposited the "triple-layer model" (Figure 1) describes the structure of the double layer developed between the suspended support particles and the impregnating solution.[13−16,25−27,39−44] Adopting this model, the following possibilities exist concerning the part of the double layer where the deposited vanadates are located: (i) the diffuse part of the double layer; (ii) the IHP in contact with the support surface.

Figure 2 illustrates the variation, with pH, of the electrokinetic charge density of the support suspension in the presence and absence of vanadate ions (curves b and a, respectively) as well

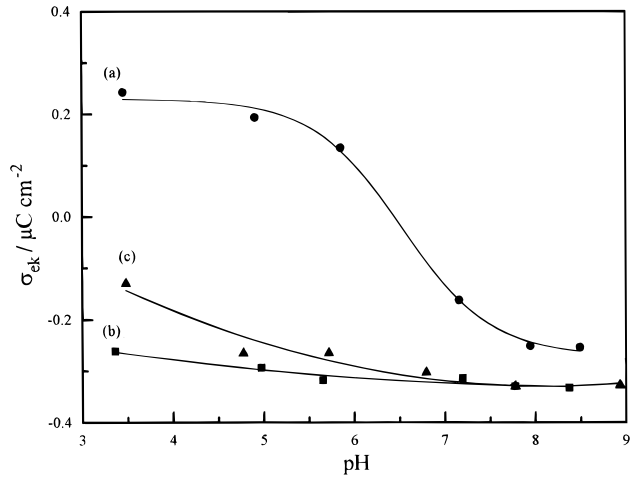

Figure 2. Variation of the electrokinetic charge of anatase and V_2O_5/TiO_2 catalyst, with the pH of the suspension at 25 °C: (a) TiO_2, I = 0.01 mol dm^{-3} NH_4NO_3 solution; (b) TiO_2, ammonium vanadate solution, $C_0 = 1.5 \times 10^{-3}$ $V^{(v)}$ mol dm^{-3}, I = 0.01 mol dm^{-3} NH_4NO_3; (c) V_2O_5/TiO_2 catalyst, I = 0.01 mol dm^{-3} NH_4NO_3 solution.

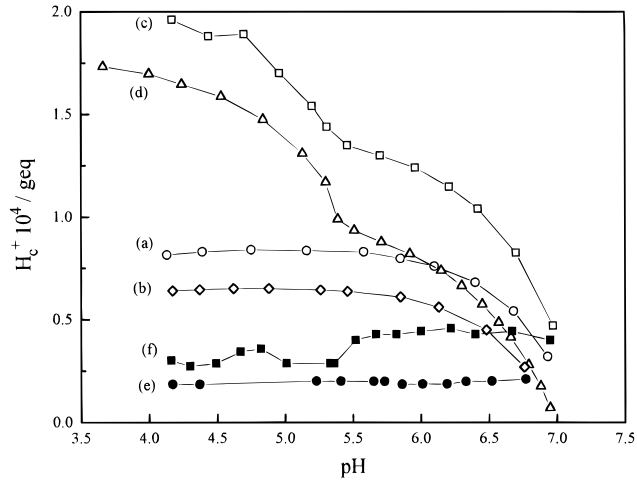

Figure 3. Hydrogen ions consumed due to the protonation of surface hydroxyls as well as due to the equilibria taking place in the solution: (a) suspension TiO_2/NH_4NO_3; (b) solution NH_4NO_3; (c) suspension $TiO_2/NH_4NO_3/H_xV_yO_z^{n-}$ ions; (d) solution $NH_4NO_3/H_xV_yO_z^{n-}$ ions. I = 0.1 mol dm^{-3}.

as of a V_2O_5/TiO_2 catalyst suspension (curve c). It should be noted that the σ_{ek} values refer to the total charge from the surface to the shear plane (Figure 1). It may be observed that the presence of the vanadates in the suspension of the support rendered the values of σ_{ek} negative over the entire pH range studied. Obviously this finding precluded the location of the negative vanadate ions as counterions in the diffuse part of the double layer because in that case the charge from the surface to the shear plane, namely, the electrokinetic charge, should be positive in order to compensate the negative charge of the vanadate ions. Therefore, one may propose that the vanadate ions are presumably located in the inner Helmholtz plane in contact with the anatase surface.

The deposition of the $V^{(v)}$ species at the IHP is expected to disturb the equilibria 2. In fact, the decrease in the free $TiOH_2^+$ groups due to the possible adsorption at the IHP of the $V^{(v)}$ negative species and the decrease in the free TiOH groups due to the possible reaction with these species are expected to cause a shift of the equilibria 2 to the left. Therefore, it is anticipated that the hydrogen ions consumed in equilibria 2, H_c^+, will be more in the presence than in the absence of the $V^{(v)}$ species in the impregnating solution. Figure 3 illustrates the variation of H_c^+, with pH, for various solutions and suspensions. Subtraction of curve b from curve a provides the variation of H_c^+ with pH due to equilibria 2 in the absence of the $V^{(v)}$ species (curve e), whereas subtraction of curve d from curve c provides the variation of H_c^+ with pH due to equilibria 2 but in the presence of the $V^{(v)}$ species (curve f). Comparison of curves f and e confirms our anticipation that the hydrogen ions consumed in equilibria 2 will be more in the presence than in the absence of the $V^{(v)}$ species, corroborating the above mentioned conclusion that these species are specifically deposited in the IHP, via electrostatic adsorption on the $TiOH_2^+$ groups or reaction with the TiOH groups.

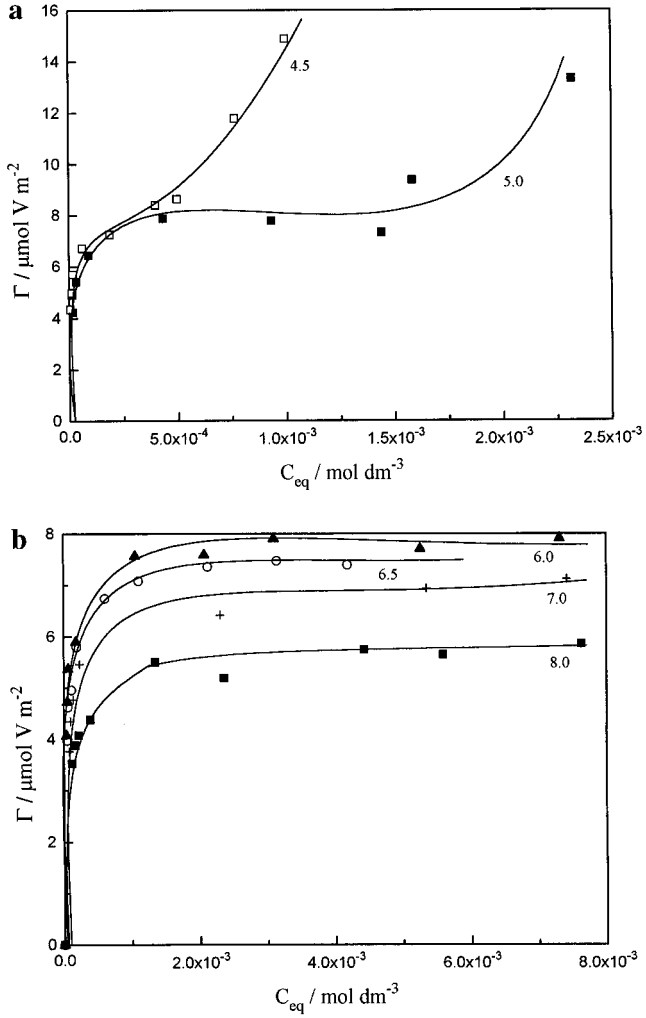

Figure 4. (a) Surface concentration of $V^{(v)}$ as a function of the equilibrium $V^{(v)}$ concentration at various pH values of the impregnating suspension. T = 25 °C, I = 0.1 mol dm^{-3} NH_4NO_3. pH values are indicated. (b) Surface concentration of $V^{(v)}$ as a function of the equilibrium $V^{(v)}$ concentration at various pH values of the impregnating suspension. T = 25 °C, I = 0.1 mol dm^{-3} NH_4NO_3. pH values are indicated.

Investigation of the Nature of the Deposition Sites. If the above mentioned conclusion concerning the mechanism of deposition of the $V^{(v)}$ species is generally correct, an increase in the extent of deposition, expressed by the value of Γ, is expected with the concentration of $TiOH_2^+$ and TiOH groups. Therefore, an increase in this extent may be anticipated as pH decreased (see equilibria 2). The deposition isotherms show that this is, in effect, the case (Figure 4a,b).

Moreover, it should be stressed the remarkable extent of deposition at relatively high pH values (pH range 6.0−8.0), where a drastic decrease of the concentration of the $TiOH_2^+$ groups occurs. This observation indicates that the contribution of the deposition via reaction with the TiOH groups should be important. This conclusion is also corroborated by the observa-

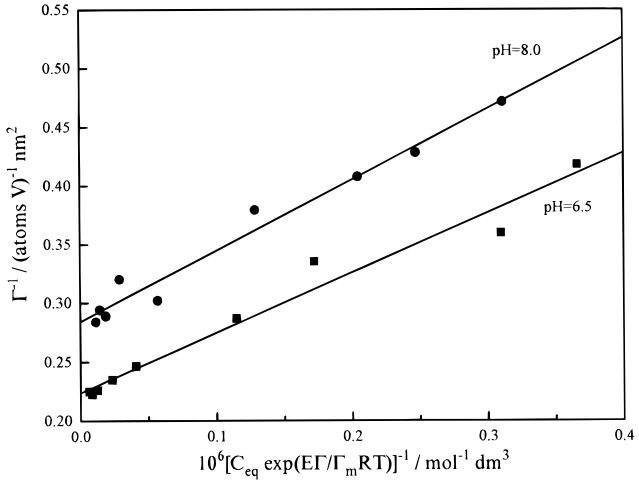

Figure 5. Reciprocal surface concentration of $V^{(v)}$ as a function of $1/C_{eq}\exp(E\Gamma/\Gamma_m RT)$ at various pH values of the impregnating suspension. The solid lines represent the values calculated usinq eq 4.

tion that the microelectrophoretic curve of the TiO_2 suspensions in the presence of the $V^{(v)}$ species is similar to that of the V_2O_5/TiO_2 suspensions over a large pH range (compare parts b and c of Figure 2). In contrast, the observation that the extent of deposition decreased with pH and thus with the concentration of the TiO^- groups strongly suggests that deposition of the negative $V^{(v)}$ species on these groups should not be considered.

The type of the deposition isotherms achieved generally suggests Langmuir deposition with weak, if any, lateral interactions between the deposited $V^{(v)}$ species.[45]

In the pH values 4.5 and 5.0, the plateau of the respective isotherms is obtained at relatively low values of C_{eq}. An abrupt increase in the values of Γ is observed above a critical C_{eq} value. This may be due to the fact that in the pH range 4.5−5.0 the $V_{10}O_{27}^{4-}$ and $HV_{10}O_{28}^{5-}$ ions are present in the impregnating solution, and thus a precipitation of these ions is very possible. In view of the above deposition may be assumed on energetically equivalent sites up to a critical C_{eq} value for pH 4.5 and 5.0 and for the whole concentration range studied for the pH values higher than 6. For these cases the "Stern−Langmuir−Fowler" equation should describe the deposition isotherms.

$$\frac{1}{\Gamma} = \frac{1}{\Gamma_m} + \frac{1}{\bar{K}\Gamma_m C_{eq}\exp\left(\frac{\bar{E}\Gamma}{\Gamma_m RT}\right)} \qquad (3)$$

In the above equation Γ, Γ_m, $\bar{K}$, C_{eq}, and $\bar{E}$ denote, respectively, the surface concentration and the saturation surface concentration of $V^{(v)}$, the deposition constant, the equilibrium concentration of $V^{(v)}$, and the energy of the lateral interactions exerted among the deposited $V^{(v)}$ species. It was found that eq 3 described satisfactorily our experimental results. Typical results are illustrated in Figure 5. These corroborate the aforementioned assumption with respect to the localized character of deposition in our case.

A Quantitative Approach to the Deposition Model

Tentative Deposition Mechanism. In order to write a tentative, quite general, mechanism for the deposition of the $V^{(v)}$−oxo species on the anatase/electrolyte solution interface, we must take into account the following: (i) the findings reported in the previous paragraphs; (ii) the deposition mechanism established for the deposition of the $Cr^{(vi)}$−oxo species and $Mo^{(vi)}$−oxo species on the surface of titania.[14,16]

In view of the above we write the following, quite general, tentative deposition mechanism.

$$\mu_i TiOH_2^+ + V^{(v)}\ \text{species}_j \leftrightarrow (TiOH_2^+)_{\mu_i} \ldots V^{(v)}\ \text{species}_j \qquad (4a)$$

$$\nu_i TiOH + V^{(v)}\ \text{species}_j \leftrightarrow Ti_{\nu_i} - V^{(v)}\ \text{species}_j + \nu_i OH^- \qquad (4b)$$

$$\mu_i TiOH_2^+ + \nu_i TiOH + V^{(v)}\ \text{species}_j \leftrightarrow Ti_{\nu_i} - V^{(v)}\ \text{species}_j \ldots (TiOH_2^+)_{\mu_i} + \nu_i OH^- \qquad (4c)$$

In the above equilibria $V^{(v)}$ species_j represent the vanadate ionic species present in the suspensions under our experimental conditions. These are considered to be located in the IHP. μ_i and ν_i denote the number of $TiOH_2^+$ and TiOH groups involved in each equilibrium.

According to this mechanism the $V^{(v)}$−oxo species are first moved from the bulk solution to the IHP following a Boltzmann relation. Then, most of them are dehydrated and adsorbed on sites at the IHP by replacing adsorbed water molecules. Adsorption occurs on a site at the IHP created by one or two adjacent $TiOH_2^+$ groups of anatase (equilibrium 4a). The $V^{(v)}$ species, being in the IHP, may be moreover deposited via reaction with one or two adjacent TiOH groups of anatase (equilibrium 4b), releasing one or two OH^- ions in the IHP. Finally, these species may be deposited by simultaneous adsorption and reaction (equilibrium 4c).

It should be mentioned that adsorption or reaction with sites created by more than two $TiOH_2^+$ or TiOH adjacent groups, respectively, has not been considered because it is not a realistic assumption. In fact, it has been shown that negligible adsorption and reaction of the $Cr^{(vi)}$−oxo and $Mo^{(vi)}$−oxo species occur on sites created even for two adjacent (protonated or neutral) surface hydroxyls of titania.[14,16] It is moreover noticeable that for the species $H_2VO_4^-$ with charge lower than 2 we don't consider adsorption or reaction with a site created by two $TiOH_2^+$ or two TiOH adjacent surface hydroxyls, respectively.

Taking into account the above and the fact that six different $V^{(v)}$ species are present in the impregnating solution, it is clear that eqs 4 describe 27 different equilibria.

Derivation of Equations That Describe the Deposition Equilibria. Following a procedure, a generalization of which has been described in ref 17, we derived the following general equation:

$$C_i = \lambda_i^{-1}\exp\left(-\frac{\Delta G^\circ_{cs,i}}{RT}\right)\exp\left(\frac{\mu_i F\Phi_0}{RT}\right)\times 10^{\nu_i(14-\text{pH})}\times \exp\left(\frac{-z_i F\Psi_{IHP}}{RT}\right)\exp\left(\frac{\bar{E}n|z_i|\Gamma}{\Gamma_m RT\sum_{i=1}^{n}|z_i|}\right)\times [V^{(v)}\ \text{species}_j]_b (C^f_{TiOH_2^+})^{\mu_i}(C^f_{TiOH})^{\nu_i} \qquad (5)$$

The subscript i corresponds to a given equilibrium. A supported $V^{(v)}$ species formed through an equilibrium i is denoted as $V^{(v)}$ species_i. In the above equation C_i, $\Delta G^\circ_{cs,i}$, F, Φ_0, Ψ_{IHP}, $\bar{E}$, n, $[V^{(v)}\ \text{species}_j]_b$, $C^f_{TiOH_2^+}$, and C^f_{TiOH} symbolize, respectively, the concentration of a $V^{(v)}$ species_i illustrated in the rhs of eqs 4a−4c, the standard free energy of the chemical interactions between the deposited $V^{(v)}$ species and the sites of the support

for an equilibrium i, the Faraday constant, the Galvani potential at the surface, the Volta potential at the IHP, the mean energy of the lateral interactions exerted among the deposited $V^{(v)}$ species, the number of the kind of these species that are formed on the support surface at a given pH, the concentration of the $V^{(v)}$ species in the bulk solution at equilibrium, and the concentration of the free (uncovered) $TiOH_2^+$ and TiOH groups. λ_i is a proportionality constant. z_i is the charge of a deposited $V^{(v)}$ species$_i$. It is obvious that $z_i = z_j + \nu_i$, where z_j is the charge of a species to be deposited. The symbols μ_i, ν_i, Γ, and Γ_m have been explained before.

Unfortunately, eq 5 cannot be used directly for the calculation of the concentration of a $V^{(v)}$ species$_i$ formed on the support surface. There are two main reasons for this. The first is that the product of the first four terms of eq 5 is unknown. However, this product is constant at a given pH. Therefore, we may write the equation

$$K_i = \lambda_i^{-1} \exp\left(-\frac{\Delta G^\circ_{cs,i}}{RT}\right) \exp\left(\frac{\mu_i F \Phi_0}{RT}\right) \times 10^{\nu_i(14-pH)} \quad (6)$$

where K_i is the deposition constant for a $V^{(v)}$ species$_i$ formed on the support surface. This constant describes the deposition from the IHP to the "final deposition state". The second reason is that the mean energy of the lateral interactions exerted among the deposited $V^{(v)}$ species, $\bar{E}$, is also unknown. It is therefore necessary to adopt an approximate procedure in order to determine the values of K_i and $\bar{E}$ and then return and use eq 5. This can be achieved by deriving an approximate equation which would be tested experimentally. The derivation of this expression is achieved following a procedure similar to, *but not identical with*, that described in ref 17. *The most important points as well as several improvements in the methodology are presented here.* The starting point is the following equation, which may be derived by transforming eq 5.

$$\frac{\Theta_i}{(1-\Theta_{TiOH_2^+})^{\mu_i}(1-\Theta_{TiOH})^{\nu_i}} = \exp\left(-\frac{\Delta G^\circ_{cs,i}}{RT}\right) \exp\left(\frac{\mu_i F \Phi_0}{RT}\right) \times 10^{\nu_i(14-pH)} \times \exp\left(\frac{-z_i F \Psi_{IHP}}{RT}\right) \exp\left(\frac{\bar{E} n |z_i| \Gamma}{\Gamma_m RT \sum_{i=1}^{n} |z_i|}\right) [V^{(v)}\ species_j]_b \quad (7)$$

In the above equation Θ_i, $\Theta_{TiOH_2^+}$, and Θ_{TiOH} symbolize, respectively, the fraction of the sites covered by a $V^{(v)}$ species$_i$, the fraction of the covered $TiOH_2^+$ groups, and the fraction of the covered TiOH groups. These fractions are defined by the following equations.

$$\Theta_i = \lambda_i \frac{C_i}{(C^t_{TiOH_2^+})^{\mu_i}(C^t_{TiOH})^{\nu_i}} \quad (8a)$$

$$\Theta_{TiOH_2^+} = \frac{C^c_{TiOH_2^+}}{C^t_{TiOH_2^+}} \quad (8b)$$

$$\Theta_{TiOH} = \frac{C^c_{TiOH}}{C^t_{TiOH}} \quad (8c)$$

In the above equations by the upperscripts t and c we denote, respectively, total (free + covered) and covered surface hydroxyl groups. λ_i is the proportionality constant mentioned before.

By replacing Θ with Γ/Γ_m, taking into account eq 6 and assuming (i) $[V^{(v)}\ species_j]_b = \alpha_j C_{eq}$ (α_j is a coefficient), (ii) $\sum_{i=1}^{27} \Theta_i/(1-\Theta_{TiOH_2^+})^{\mu_i}(1-\Theta_{TiOH})^{\nu_i}] \cong \Theta/(1-\Theta)$, we added eqs 7 and derived the simplified eq 9 in which both Γ and C_{eq} may be determined experimentally.

$$\frac{1}{\Gamma} = \frac{1}{\Gamma_m} + \frac{1}{\Gamma_m C_{eq} \sum_{i,j} K_i \alpha_j \exp\left(\frac{-z_i F \Psi_{IHP}}{RT}\right) \exp\left(\frac{\bar{E}\Gamma |z_i| n}{\Gamma_m RT \sum_{i=1}^{n} |z_i|}\right)} \quad (9)$$

By comparing eq 9 with the corresponding eq 38 of ref 17 (where our methodology had been presented), one can easily notice the improvements achieved. Specifically three assumptions necessary for deriving eq 38 of ref 17 have been eliminated. First, the deposition constants, K_i, (see eq 6) do not involve the term $\exp(-z_i F \Psi_{IHP}/RT)$ as it had been assumed in ref 17. Second, E_i is not assumed to be equal to $\bar{E}$ for any value of i, but it depends on the charge of the deposited species. Third, the coefficient a_j is not assumed to be independent of C_{eq}. On the contrary, it is considered to be strongly dependent on the $V^{(v)}$ concentration in the bulk solution, in agreement with our observations. The improved and more accurate eq 9 as it is compared with the eq 38 of ref 17 may be treated by applying a fitting program described in the next paragraph. Moreover, it may be tested experimentally.

Adopting several assumptions concerning the relationships between the K_i values (see ref 17), eq 9 can be transformed to a similar equation, involving only two constants, K_i. We symbolize these two constants by K_A and K_R. These correspond, respectively, to the adsorption of the $H_2VO_4^-$ species on a $TiOH_2^+$ group and to the reaction of these species with a TiOH group. The application, *for the first time*, of a fitting program (FP)[46] allowed us to fit our experimental data (Γ, C_{eq}), to eq 9 and calculate the constants K_A, K_R, and thus K_i, as well as the mean energy of the lateral interactions, $\bar{E}$. All the terms of eq 9 are known except the Volta potential at the IHP, Ψ_{IHP}. However, having known the value of Ψ_{IHP} from previous systems[14,16] in a wide pH and concentration range, it is quite easy to insert into the program conjectured values of Ψ_{IHP} very close to the final ones.

Calculations in the Suspension and Elucidation of the Deposition Mechanism. Adoption of a calculating procedure using the computer program SURFEQL, which is described in detail in ref 17, allowed us to calculate the following parameters, at a given pH: (i) the concentrations of the $V^{(v)}$−oxo species in the bulk solution (see Table 1) and thus the value of C_{eq} and (ii) the deposition constants, K_i, of the surface complexes which actually contribute to the whole deposition (see Table 2) among those illustrated in the rhs of equilibria 4 as well as their concentrations, Γ_i, and thus the total surface concentration, Γ, for the deposited $V^{(v)}$. Figure 6 illustrates a typical example at pH = 8.0. The achievement of the very good agreement between the calculated and experimental Γ *vs* C_{eq} isotherms strongly suggests that the values of Γ_i used for calculating the values of Γ as well as the tentative deposition mechanism are correct. The assumption of an "incorrect" mechanistic model does not permit such good agreement. It should be stressed here that this agreement is achieved in the entire pH range studied, 4.5−8.0.

TABLE 2: Values of the Deposition Constants at Different pH Values

pH	K_1	K_2	K_3	K_4	K_5	K_6	K_7	K_8	K_9	K_{10}	K_{11}	K_{12}
4.5	6.0×10^4	6.0×10^4	6.0×10^4		3.1×10^{-7}	3.1×10^{-7}	9.9×10^{-14}	3.1×10^{-7}	9.9×10^{-14}			
5.0	6.4×10^4			6.4×10^5	1.0×10^{-6}		1.0×10^{-12}		1.0×10^{-12}	1.0×10^{-6}	1.0×10^{-12}	
6.0	2.5×10^5			2.5×10^6	8.0×10^{-6}					8.0×10^{-6}	6.4×10^{-11}	
6.5	4.2×10^5			4.2×10^6	3.2×10^{-5}					3.2×10^{-5}	1.0×10^{-9}	
7.0	5.0×10^5			5.0×10^6	9.0×10^{-5}						8.1×10^{-9}	
8.0	3.5×10^6				7.0×10^{-4}						4.9×10^{-7}	4.9×10^{-7}

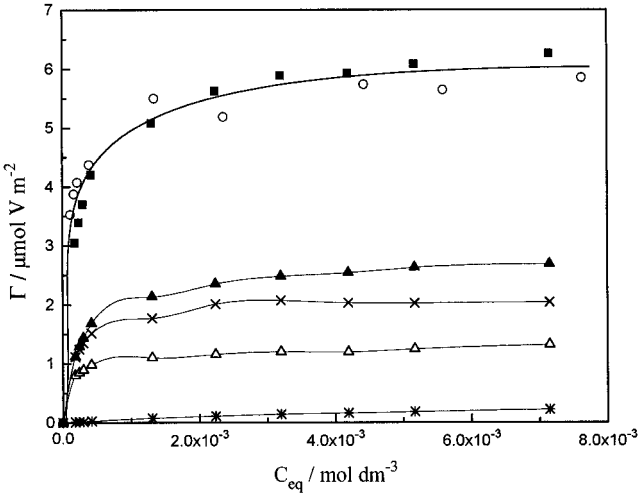

Figure 6. Variation of the surface concentration of $V^{(v)}$ with the equilibrium $V^{(v)}$ concentration: experimental (○) and calculated (■) isotherm for the total $V^{(v)}$ deposition on the anatase surface. Symbols △, ▲, ×, and * correspond, respectively, to the calculated isotherms for the $V^{(v)}$ deposition through adsorption of one $H_2VO_4^-$ ion on a site created by one $TiOH_2^+$ group, through reaction of one $H_2VO_4^-$ ion with one TiOH group, through reaction of one HVO_4^{2-} ion with two adjacent TiOH groups, and through reaction of one $V_3O_9^{3-}$ ion with two adjacent TiOH groups. pH = 8.0, $T = 25$ °C, $I = 0.1$ M NH_4NO_3.

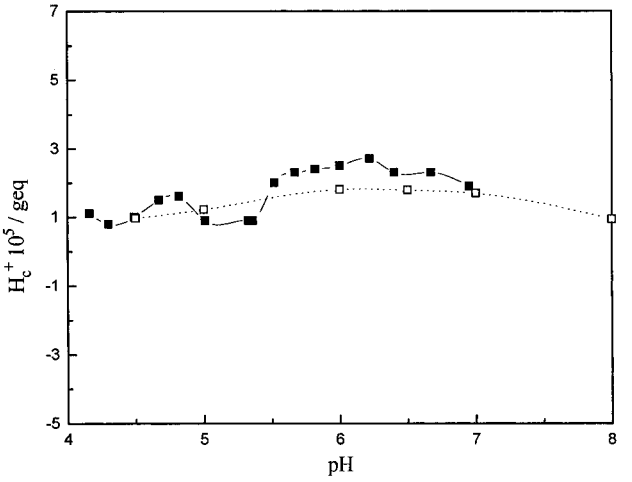

Figure 7. Variation of ΔH_c^+ with pH: ΔH_c^+(experimental) (■); ΔH_c^+(calculated) (□) (see text). $T = 25$ °C, $I = 0.1$ M NH_4NO_3.

(iii) On the basis of the established deposition mechanism we calculated, using SURFEQL, in the pH range studied, the amount $\Delta H_c^+ = \Delta([TiOH_2^+] - [TiO^-])_t$, which expresses the difference of the hydrogen ions consumed on the anatase surface, in the presence and absence of the $V^{(v)}$ species in the suspension. The variation of ΔH_c^+ with pH ($\Delta H_c^+ = H_c^+$(in the presence of $V^{(v)}$ species) $- H_c^+$(in the absence of $V^{(v)}$ species)) may be determined experimentally. The achievement of an agreement between the calculated and experimental ΔH^+ *vs* pH curves (Figure 7) corroborates the above established deposition mechanism.

(iv) In the final step of the title procedure we calculated, using SURFEQL and taking into account the established mechanism, the variation, with pH, of the Volta potential at the shear plane of the double layer, Ψ_d, which is assumed to be equal to the ζ-potential. This may also be determined by microelectrophoretic mobility measurements in the presence of $V^{(v)}$ species in the suspension. The quite good agreement achieved between the experimental and calculated ζ *vs* pH curves (Figure 8) confirms the above inferred deposition model.

Results and Discussion

The Real Deposition Mechanism. Following the above described procedure, we found that among the 27 equilibria tentatively assumed (equilibria 4) only 12 contribute actually to the whole deposition. Consequently, the deposition mechanism, proposed before, may be significantly simplified into

$$TiOH_2^+ + H_2VO_4^- \overset{K_1}{\longleftrightarrow} TiOH_2^+\cdots H_2VO_4^- \quad (10a)$$

$$TiOH_2^+ + V_{10}O_{27}^{4-} \overset{K_2}{\longleftrightarrow} TiOH_2^+\cdots V_{10}O_{27}^{4-} \quad (10b)$$

$$TiOH_2^+ + HV_{10}O_{28}^{5-} \overset{K_3}{\longleftrightarrow} TiOH_2^+\cdots HV_{10}O_{28}^{5-} \quad (10c)$$

$$TiOH_2^+ + V_3O_9^{3-} \overset{K_4}{\longleftrightarrow} TiOH_2^+\cdots V_3O_9^{4-} \quad (10d)$$

$$TiOH + H_2VO_4^- \overset{K_5}{\longleftrightarrow} TiH_2VO_4 + OH^- \quad (10e)$$

$$TiOH + V_{10}O_{27}^{4-} \overset{K_6}{\longleftrightarrow} TiV_{10}O_{27}^{3-} + OH^- \quad (10f)$$

$$2TiOH + V_{10}O_{27}^{4-} \overset{K_7}{\longleftrightarrow} Ti_2V_2O_{27}^{2-} + 2OH^- \quad (10g)$$

$$TiOH + HV_{10}O_{28}^{5-} \overset{K_8}{\longleftrightarrow} TiHV_{10}O_{28}^{4-} + OH^- \quad (10h)$$

$$2TiOH + HV_{10}O_{28}^{5-} \overset{K_9}{\longleftrightarrow} Ti_2HV_{10}O_{28}^{3-} + 2OH^- \quad (10i)$$

$$TiOH + V_3O_9^{3-} \overset{K_{10}}{\longleftrightarrow} TiV_3O_9^{2-} + OH^- \quad (10j)$$

$$2TiOH + V_3O_9^{3-} \overset{K_{11}}{\longleftrightarrow} Ti_2V_3O_9^- + 2OH^- \quad (10k)$$

$$2TiOH + HVO_4^{2-} \overset{K_{12}}{\longleftrightarrow} Ti_2HVO_4 + 2OH^- \quad (10l)$$

Moreover, the procedure mentioned before allowed us to calculate, over the entire pH range studied, the concentration of each of the $V^{(v)}$ species$_i$ illustrated in the rhs of equilibria 10 and plot the corresponding isotherms. An example for pH = 8.0 is illustrated in Figure 6, where it may be seen the calculated isotherms corresponding to equilibria 10a, 10e, 10k, and 10l. At this pH the other equilibria do not practically contribute to the deposition, and this is the reason that the corresponding calculated isotherms are not presented. Inspection of Figure 6 shows the importance of the contribution of the chemical reaction of the $H_2VO_4^-$ and HVO_4^{2-} ions with the neutral surface hydroxyls to the whole deposition. The participation of these hydroxyls to the whole deposition had been already inferred by the observations mentioned in the previous section, Investigation of Nature of the Deposition Sites. As we shall

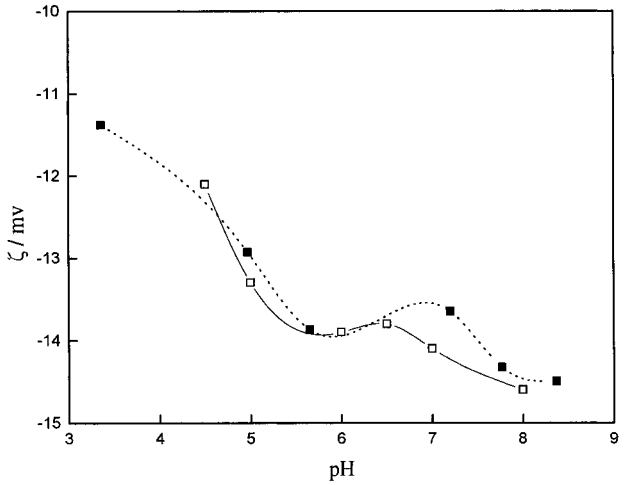

Figure 8. Variation of the ζ-potential, with pH, in the presence of $V^{(v)}$ species: (■) experimental values; (□) calculated values. $T = 25$ °C, $I = 0.01$ M NH_4NO_3.

see later, this participation is important in the whole pH range (see Figure 9a,b).

Let us return to the aforementioned deposition mechanism (equilibria 10). The most important observation is that this mechanism is quite complicated. Figure 9a,b illustrates the variation, with pH, of the surface concentration of each of the $V^{(v)}$ species formed on the anatase surface, for high and low $[V^{(v)}]_t$ values, respectively. It may be observed that in Figure 9a (9b) nine (five) equilibria contribute to the whole deposition curves.

A second important observation *is the selective deposition*, in the entire pH range, of the monomeric $V^{(v)}$ species ($H_2VO_4^-$, HVO_4^{2-}) with respect to the polymeric ones ($V_3O_9^{3-}$, $V_4O_{12}^{4-}$, $V_{10}O_{27}^{4-}$, $HV_{10}O_{28}^{5-}$). In fact, inspection of Figure 9a shows that the $V_{10}O_{27}^{4-}$ and $HV_{10}O_{28}^{5-}$ ions are deposited only in the pH range 4.5−5.0 mainly via adsorption on a $TiOH_2^+$ group or via reaction with two adjacent TiOH groups. As to the $V_3O_9^{3-}$ ions, these are deposited via adsorption on a $TiOH_2^+$ group or via reaction with two adjacent TiOH groups in the pH range 5.0−8.0. On the other hand the deposition of the $V_4O_{12}^{4-}$ ions is negligible in the entire pH range. Finally, the absence of the species $V_{10}O_{27}^{4-}$ and $HV_{10}O_{28}^{5-}$ in Figure 9b as well as the low participation of the $V_3O_9^{3-}$ ions in the whole deposition can be noticed.

A third remarkable observation is the relatively high coverage of the surface of anatase (see Table 3). Especially, the coverage of the protonated surface hydroxyls, $TiOH_2^+$, ranges between 71% and 89% over the pH range 4.5−8.0. It can be observed that the deposition through adsorption predominates at low pH values. The coverage of the neutral hydroxyls, TiOH, is also sufficiently high and ranges between 12% and 37% over the entire pH range 4.5−8.0 (see Table 3). This shows the strong chemical affinity between the $V^{(v)}$ species and the surface of anatase. It may observed that the deposition via reaction predominates at relatively high pH values.

The Factors That Determine the Extent of Deposition. In order to explain the observations mentioned in the previous section, we must recall eq 5, which describes the deposition of a $V^{(v)}$ species$_i$. The finding that the deposition mechanism is quite complicated could be easily attributed to the fact that a variation of pH or in the total $V^{(v)}$ concentration, $[V^{(v)}]_t$, causes extensive changes in the relative concentrations of the $V^{(v)}$ species in the bulk solution (see Table 1).

Let us now explain the selective deposition of the monomeric species ($H_2VO_4^-$, HVO_4^{2-}). The first reason for this selectivity is that the concentrations of these species are relatively high in

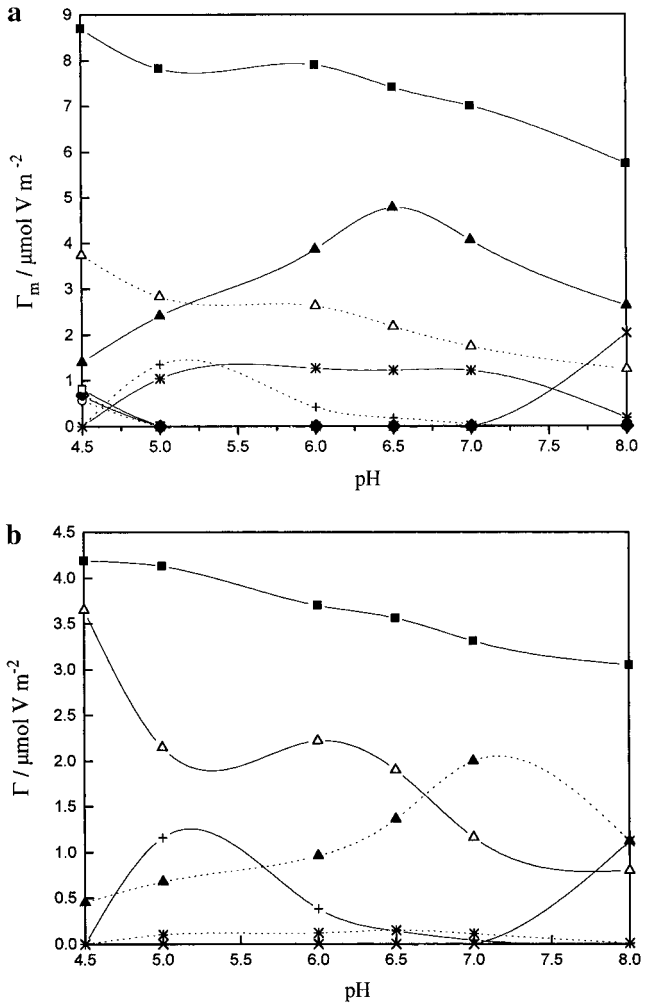

Figure 9. (a) Variation, with pH, of the maximum amount of $V^{(v)}$ deposited on the anatase surface through adsorption, on a site created by one $TiOH_2^+$ group, of one $H_2VO_4^-$ (△), $V_3O_9^{3-}$ (+), $V_{10}O_{27}^{4-}$ (◇), and $HV_{10}O_{28}^{5-}$ (○) ion, through reaction with a TiOH group of one $H_2VO_4^-$ (▲) ion, and through reaction with two adjacent TiOH groups of one HVO_4^{2-} (×), $V_3O_9^{3-}$ (*), $V_{10}O_{27}^{4-}$ (□), and $HV_{10}O_{28}^{5-}$ (●) ion. The variation of Γ_m with pH for the total amount of $V^{(v)}$ is also indicated (■). (b) Variation, with pH, of the amount of $V^{(v)}$ deposited on the anatase surface through various modes of deposition. Symbols as in part a. $C_0 = 6 \times 10^{-4}$ $V^{(v)}$ mol dm^{-3}.

TABLE 3: Values of Various Ratios That Illustrate the Coverage of the Surface Hydroxyls of the Anatase Surface Calculated at Various pH[a,b,c]

pH	$\frac{[TiOH_2^+]_c}{[TiOH_2^+]_f + [TiOH_2^+]_c}$	$\frac{[TiOH]_c}{[TiOH]_f + [TiOH]_c}$	$\frac{[TiOH]_c + [TiOH_2^+]_c}{[TiOH]_f + [TiOH]_c + [TiOH_2^+]_f + [TiOH_2^+]_c}$
4.5	0.79	0.12	0.28
5.0	0.71	0.21	0.32
6.0	0.80	0.29	0.38
6.5	0.81	0.33	0.40
7.0	0.81	0.28	0.33
8.0	0.89	0.37	0.41

[a] The values correspond to the plateau of the respective isotherms. [b] f: free. [c] c: covered.

the bulk solution (see Table 1). A second reason is that the amount $\exp(-z_i F\Psi_{IHP}/RT)$ (see eq 5) decreased dramatically as $|z_i|$ increased, bringing about a decrease in the concentration of the species$_i$ with relatively high negative charge at the IHP and then, through eq 5, in the final deposition state. This occurs because the negatively charged $V^{(v)}$ species should be first located in the IHP where the potential, Ψ_{IHP}, is also negative. The above simply reflects the fact that the deposition of species with relatively high negative charge (polymeric species) on a

negatively charged plane is quite difficult. Another very important factor that favors the deposition of the species with low charge (monomeric species) is related to the amount $\exp(\bar{E}|z_i|n\Gamma/\Gamma_m RT\sum_{i=1}^{n}|z_i|)$ (see eq 5). In contrast to recent findings concerning the deposition of $Cr^{(vi)}$−oxo species and $Mo^{(vi)}$−oxo species on titania,[14,16] in our case the values of the mean energy of lateral interactions, $\bar{E}$, are negative in the entire pH range studied. Thus, an increase of $|z_i|$ causes a decrease in the aforementioned amount, thus inhibiting the deposition of the polymeric species. The influence of the negative $\bar{E}$ is more pronounced in the equilibrium concentrations corresponding to the plateau of the isotherms where these species have considerable concentration in the bulk solution.

The observed tendency for deposition through adsorption (reaction) at relatively low (high) pH may be easily attributed to the increase of the concentration of the $TiOH_2^+$ (TiOH) groups as pH decreased (increased) (see eq 6).

Moreover, the observation that the adsorption is a very strong and selective process and takes place even at high pH values where the concentration of the $TiOH_2^+$ groups is very low can be attributed to the quite high values of K_i's related with the adsorption equilibria (K_1, ..., K_4 constants, Table 2).

A last point that we have to explain is the lack of contribution to the whole deposition of the equilibria which involve two adjacent $TiOH_2^+$ groups or the $TiOH_2^+$−O−TiOH groups. This is understandable if we take into account that $C^f_{TiOH_2^+}$ is much lower than unity and thus $(C^f_{TiOH_2^+})^2 << C^f_{TiOH_2^+}$ and $C^f_{TiOH_2^+}C^f_{TiOH} << C^f_{TiOH}$ (see eq 5). In contrast, we have observed that the deposition via reaction takes place almost exclusively through reaction with two adjacent TiOH groups. This may be explained if we take into account that the K_i constants for deposition on two adjacent TiOH groups (K_7, K_9, K_{11}, K_{12}) are much higher than the corresponding ones concerning the deposition on a single TiOH group (K_6, K_8, K_{10}) as well as the relatively low negative charge, z_i, of the surface species involving two adjacent TiOH groups. As we have already mentioned, the high negatively charged species are inhibited from deposition due to the two important reasons noticed before.

Conclusions

The improvement of a calculation procedure, which had been recently presented,[17] allowed us to overcome some difficulties related with the dramatic change in the composition of the vanadate solution with its concentration in $V^{(v)}$ and to investigate the mechanism of deposition of $V^{(v)}$−oxo species on the anatase surface, using a relatively small number of assumptions. The most important findings concerning this mechanism may be summarized as follows.

(i) The mechanism of deposition of the $V^{(v)}$−oxo species on the surface of anatase is quite complicated. Thus, 12 equilibria are needed to describe the title deposition.

(ii) A preference was found for the deposition of the monomeric with respect to the deposition of the polymeric $V^{(v)}$−oxo species.

(iii) The deposition through adsorption (reaction) is favored at relatively low (high) pH values on (with) sites created by single $TiOH_2^+$ (TiOH) groups.

(iv) No significant deposition has been observed on two adjacent $TiOH_2^+$ groups or $TiOH_2^+$−O−TiOH groups.

(v) The above findings may be easily explained on the basis of an equation derived adopting the "two-p*K*/one-site" and the triple-layer models.

Acknowledgment. Financial support to K.B. and I.G. from the Greek Award Granting Authority (IKY) is gratefully acknowledged.

References and Notes

(1) Bosch, H.; Janssen, F. *Catal. Today* **1988**, *2*, 369.
(2) Nakatsuji, T.; Miyamoto, A. *Catal. Today* **1991**, *10*, 21.
(3) Topsøe, N.-Y.; Topsøe, H.; Dumesic, J. A. *J. Catal.* **1995**, *151*, 226.
(4) Ciambelli, P.; Lisi, L.; Russo, G.; Volta, J. C. *Appl. Catal*. **1995**, *7*, 1.
(5) Machej, T.; Haber, J.; Turek, A. M.; Wachs, I. E. *Appl. Catal*. **1991**, *70*, 115.
(6) Roozeboom, E.; Mittelmeijer-Hazeleger, M. C.; Moulijn, J. A.; Medema, J.; de Beer, V. H. J.; Gellings, P. J. *J. Phys. Chem*. **1980**, *84*, 2783.
(7) Kantcheva, M.; Davydov, A.; Hadjivanov, K. *J. Mol. Catal*. **1993**, *81*, L25.
(8) Kantcheva, M.; Bushev, V.; Klissurski, D. *J. Catal*. **1994**, *145*, 96.
(9) Kantcheva, M. M.; Hadjivanov, K. I.; Klissurski, D. *J. Catal*. **1992**, *134*, 299.
(10) Spanos, N.; Slavov, S.; Kordulis, Ch.; Lycourghiotis, A. *Langmuir* **1994**, *10*, 3134.
(11) Spanos, N.; Lycourghiotis, A. *Langmuir* **1994**, *10*, 2351.
(12) Karakonstantis, L.; Bourikas, K.; Lycourghiotis, A. *J. Catal*. **1996**, *162*, 295.
(13) Spanos, N.; Slavov, S.; Kordulis, Ch.; Lycourghiotis, A. *Colloids Surf.* **1995**, *97*, 109.
(14) Bourikas, K.; Spanos, N.; Lycourghiotis, A. *Langmuir* **1997**, *13*, 435.
(15) Spanos, N.; Lycourghiotis, A. *J. Catal*. **1994**, *147*, 57.
(16) Bourikas, K.; Spanos, N.; Lycourghiotis, A. *J. Colloid Interface Sci*. **1996**, *184*, 301.
(17) Bourikas, K.; Matralis, H. K.; Kordulis, Ch.; Lycourghiotis, A. *J. Phys. Chem*. **1996**, *100*, 11711.
(18) Hiemstra, T.; Van Riemsdijk, W. H.; Bolt, G. H. *J. Colloid Interface Sci*. **1989**, *133*, 91.
(19) Hiemstra, T.; Venema, P.; Van Riemsdijk, W. H. *J. Colloid Interface Sci*. **1996**, *184*, 680.
(20) Contescu, C.; Jagiello, J.; Schwarz, J. *Langmuir* **1993**, *9*, 1754.
(21) Contescu, C.; Popa, V.; Schwarz, J. *J. Colloid Interface Sci*. **1996**, *180*, 149.
(22) Spanos, N.; Georgiadou, I.; Lycourghiotis, A. *J. Colloid Interface Sci*. **1995**, *172*, 374.
(23) Georgiadou, I.; Spanos, N.; Papadopoulou, Ch.; Matralis, H. K.; Kordulis, Ch.; Lycourghiotis, A. *Colloids Surf.* **1995**, *98*, 155.
(24) Vordonis, L.; Koutsoukos, P. G.; Lycourghiotis, A. *Colloids Surf*. **1990**, *50*, 353.
(25) Spanos, N.; Vordonis, L.; Kordulis, Ch.; Lycourghiotis, A. *J. Catal*. **1990**, *124*, 301.
(26) Vordonis, L.; Koutsoukos, P. G.; Lycourghiotis, A. *J. Catal*. **1986**, *98*, 296.
(27) Vordonis, L.; Koutsoukos, P. G.; Lycourghiotis, A. *J. Catal*. **1986**, *101*, 186.
(28) Akratopulu, K.; Vordonis, L.; Lycourghiotis, A. *J. Chem. Soc., Faraday Trans*. **1986**, *1*, 3697.
(29) Vordonis, L.; Koutsoukos, P. G.; Lycourghiotis, A. *Langmuir* **1986**, *2*, 281.
(30) Spanos, N.; Matralis, H. K.; Kordulis, Ch.; Lycourghiotis, A. *J. Catal*. **1992**, *136*, 432.
(31) Vordonis, L.; Spanos, N.; Koutsoukos, P. G.; Lycourghiotis, A. *Langmuir* **1992**, *8*, 1736.
(32) Snell, F. D. In *Photometric and Fluorometric Methods of Analysis of Metals*; Wiley: New York, 1978; Vol. 2, p 1235.
(33) Smith, R. M.; Martell, A. E. *Critical Stability Constants*; Plenum: New York, 1981; Vol. 4.
(34) Bailar, J. C.; et al. *Comprehensive Inorganic Chemistry*; Pergamon Press Ltd.: New York, 1973; Vols. 3, 4.
(35) Faughnan, J. *SURFEQL. An Interactive Code for the Calculation of Chemical Equilibria in Aqueous Systems*; W. K. Keck Laboratories 138−78, California Institute of Technology: Pasadena, CA, 1981.
(36) Huang, C. P.; Stumn, W. *J. Colloid Interface Sci*. **1973**, *43*, 409.
(37) Healy, T. W.; White, L. R. *Adv. Colloid Interface Sci*. **1978**, *9*, 303.
(38) Rudzinski, W.; Charmas, R.; Partyka, S. *Langmuir* **1991**, *7*, 354.
(39) Rudzinski, W.; Charmas, R.; Partyka, S.; Bottero, J. Y. *Langmuir* **1993**, *9*, 2641.
(40) Davis, J. A.; Leckie, J. O. *J. Colloid Interface Sci*. **1978**, *67*, 90.
(41) Davis, J. A.; James, R. O.; Leckie, J. O. *J. Colloid Interface Sci*. **1978**, *63*, 480.
(42) Davis, J. A.; Leckie, J. O. *J. Colloid Interface Sci*. **1980**, *74*, 32.
(43) Davis, J. A.; Leckie, J. O. *Chemical Modelling in Aqueous Systems*; Jenne, E. A., Ed.; American Chemical Society: Washington, DC, 1979; Chapter 15.
(44) Hiemstra, T.; De Wit, J. C. M.; Van Riemsdijk, W. H. *J. Colloid Interface Sci*. **1989**, *133*, 105.
(45) Giles, C. H.; Smith, D.; Huitson, A. *J. Colloid Interface Sci*. **1974**, *47*, 755.
(46) Aristides Zdetsis, Ph.D. Thesis, Thomas Jefferson University, Swarthmore, PA, 1976.